Position and Velocity Profile Tracking Control for New Generation Servo Track Writing

Youngwoo Lee * **Sang Hyun Kim** * **Seung-Hi Lee** ***
Chung Woo Lee ** **Chung Choo Chung**† ***

* *Department of Electrical Engineering, Hanyang University, Seoul,*
Korea (e-mail: stork@hanyang.ac.kr, eltmvpf@hanyang.ac.kr)
** *Advanced STW Development, Seagate Korea Design Center, Yongin,*
Kyunggi-do, Korea (e-mail: chungwoo.lee@seagate.com)
*** *Division of Electrical and Biomedical Engineering, Hanyang*
University, Seoul, Korea (e-mail: shlee@ieee.org,
cchung@hanyang.ac.kr)

Abstract: In this paper, we propose a new control scheme, position and velocity profile tracking control for new generation servo track writing (STW). While conventional servo track writers need controllers that perform fast positioning control with fast track seek and regulation, spiral servo track writers require accurate position and velocity profile tracking control for high quality servo patterns on the media disk. Since STW timing eventually renders geometrically accurate servo patterns, in constant velocity region both position and and velocity error signals should be regulated within small bounds. It is known that regulation via integral sliding mode controller (SMC) provides a good tracking performance, but using a high switching gain is not appropriate for a system having resonance modes. In this paper, thus we apply sliding mode control with disturbance observer to STW. To verify utility of the proposed position/velocity profile track control, we conducted some experiments using a state-of-the-art STW system. Comparative study with the conventional control method was made. The performance of proposed method was experimentally validated.

Keywords: Servo Track Writer, Sliding Mode Control, Disturbance Observer

1. INTRODUCTION

Servo track writing (STW) becomes one of the most important processes in the drive industry (Abramovitch and Franklin (2002); Mamun et al. (2007)). STW is the most time consuming process in disk drive manufacturing. Most conventional STW technologies requiring unacceptable long STW time have been becoming obsolete. New STW technologies such as spiral writing have been introduced to come up with fast (semi-self) STW. Such new STW technologies require new control methods very different technologies from the ones used for conventional STW control. While conventional servo track writers need controllers that perform fast positioning control with fast track seek and regulation, some new servo track writers require accurate position and velocity profile tracking control for high quality servo patterns on the media disk. In the latter case, STW timing eventually renders geometrically accurate servo patterns.

Unlike the conventional hard disk drives(HDDs) where point-to-point seeking performance is critical, STW using spiral servo patterning requires different type of settling performance. For advanced STW using spiral servo patterning, fast settling time to a constant velocity becomes an important specification for high performance STW to increase disk drive productivity. In constant velocity region, both position error signal (PES) and velocity error signal (VES) should be regulated within small bounds so that both PES and VES should be well controlled even before the head reaches the constant velocity region.

In this paper, we propose a new control scheme, position and velocity profile tracking control for new generation servo track writing. The proposed control scheme is implemented using sliding mode controller (SMC) with disturbance observer (DOB). Regulation via integral SMC is used for the proposed control scheme (Khalil (2002)). The add-on type DOB (Kang et al. (2011)) is used to estimate the disturbance caused by model uncertainties including resonance modes, viscous damping, etc. Comparative study with the conventional control method using PID controller in the feedback loop and feedforward control was made. It turns out that the proposed control scheme enhances settling time to the constant velocity region and further improves regulation performance of PES and VES during the constant velocity region. In addition, less oscillation in control input was observed compared to conventional method in acceleration and deceleration periods. The performance of proposed method was experimentally validated with comparisons with conventional method.

★ †: Corresponding Author
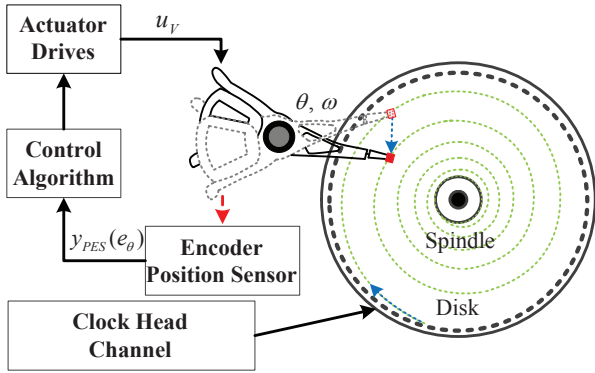
Fig. 1. Description of spiral servo track writing
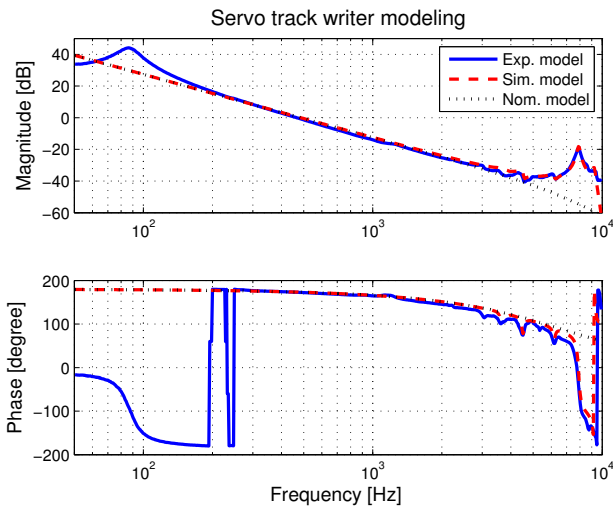
Fig. 2. Frequency response characteristics of VCM

2. MODELING AND PROBLEM DESCRIPTION

2.1 Modeling

In this section, we present the dynamical model of the actuator used in STW for spiral servo track writing depicted in Fig. 1. The actuator consists of a voice-coil motor (VCM), a sinusoidal optical encoder, and a head. The controlled variables are the position and velocity of the head. The simple nominal dynamical model of VCM actuator can be represented as a second-order rigid body in the state-space as follows:

$$\begin{bmatrix} \dot{\theta} \\ \dot{\omega} \end{bmatrix} = \underbrace{\begin{bmatrix} 0 & 1 \\ 0 & 0 \end{bmatrix}}_{A} \begin{bmatrix} \theta \\ \omega \end{bmatrix} + \underbrace{\begin{bmatrix} 0 \\ \dfrac{K_a K_t}{J_m} \end{bmatrix}}_{B} i$$

$$y = \underbrace{\begin{bmatrix} 1 & 0 \end{bmatrix}}_{C} \begin{bmatrix} \theta \\ \omega \end{bmatrix} \tag{1}$$

where θ and ω are the position and velocity of the actuator, respectively. K_a is a gain including a servo amplifier gain, the arm length of head, and the interpolator gain of sinusoidal encoder as well as A/D and D/A converters. K_t and J_m are the torque constant and the moment of inertia of the actuator mass, respectively. Driving current i is considered as the actuator input. Then,
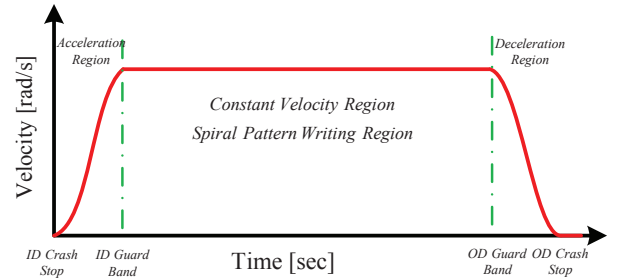
Fig. 3. Velocity profile: desired motion for the ω in Fig. 1

the transfer function, $P(s)$ from the actuator input, $I(s)$ to the actuator output, $Y(s)$ is represented by

$$\frac{Y(s)}{I(s)} := P(s) = \frac{K_a K_t}{J_m s^2} \tag{2}$$

where $I(s)$ and $Y(s)$ are the Laplace transforms of $i(t)$ and $y(t)$, respectively. However, we should consider high frequency resonance models for realistic plant model. In conventional control design approach, we use the frequency response of the actuator as illustrated in Fig. 2. Experiment model is an experimentally measured frequency response using a dynamic signal analyzer program. Simulation model is a curve fitting model obtained by system identification toolbox. Nominal model is the response for second order rigid body model (2). To suppress resonance modes in high frequency in track following mode of HDDs, it is a common approach to use gain stabilization with notch filters or phase stabilization (Yamaguchi et al. (2011); Kim et al. (2013)). In seeking mode various different approaches such as finite state control and perfect tracking control have been proposed (Yamaguchi et al. (2011)). It is practical to design velocity profile considering a second order rigid body model (1). But the velocity profile should be designed such that frequency components of the control signal around the resonance modes should be reduced not to excite them (Yamaguchi et al. (2011); Kang et al. (2011)).

2.2 Problem Description

A typical velocity profile used in spiral pattern writing is illustrated in Fig. 3. It is required to reduce the time to reach the constant velocity before the ID guard band as fast as possible. Once the head reaches the target velocity, both PES and VES should be regulated within some bounds. In this paper, therefore we use integral type sliding mode controller to reduce VES as well as PES (Khalil (2002)). In the conventional SMC, equivalent control is designed in such a way that the trajectory stays within an invariant manifold (sliding manifold) once it reaches the manifold. The reaching condition required for the convergence to a sliding manifold is ensured by the nonlinear switching function which normally has a high gain enough to reject model uncertainty as long as model uncertainty belongs to the range space of input matrice, B of (1) (Edwards and Spurgeon (1998)). However, such high gain switching results in excitation of resonance modes in high frequency, and therefore in the presence of resonance modes we cannot generally guarantee good tracking performance even though the states of (1) is near the sliding manifold. As shown in Fig. 2, the actuator

has resonance modes in high frequency near the zero dB crossover frequency of the compensated loop transfer function. In addition, there exist uncertainties such as viscous damping from ball bearings, and stiffness of flex cable effect. In general estimating such uncertainties is not easy task. In applying SMC to a dynamic system containing model uncertainties in high frequency, it is desirable to use small switching gain as much as possible by obtaining good estimation of disturbances.

3. CONTROLLER DESIGN

3.1 Error Dynamics

From the rigid body model (1), one can derive error dynamics as follows

$$\dot{e}_\theta = e_\omega$$
$$\dot{e}_\omega = \dot{\omega}^d - \frac{K_a K_t}{J_m} u \qquad (3)$$

where $e_\theta = \theta^d - \theta$, $e_\omega = \omega^d - \omega$, and u is defined as the input, i to the VCM actuator θ^d and ω^d are the desired position and velocity, respectively. Considering the uncertain and unmodeled disturbances as current equivalent disturbance, d, we can get the modified error dynamics model such as

$$\dot{e}_\theta = e_\omega$$
$$\dot{e}_\omega = \dot{\omega}^d - \frac{K_a K_t}{J_m}(u + d). \qquad (4)$$

If resonance modes are not excited, we may model the disturbance as $d = d_1 \omega + d_2$, d_1 and d_2 are unknown parameter relate to viscous damping and flex cable, respectively.

3.2 Sliding Mode Controller Design

In this section, we will explain the proposed SMC law. Equivalent control law is calculated by maintaining the ideal sliding mode. In order to track a reference trajectory, we are to develop a sliding function as follows (Khalil (2002))

$$S(e_z, e_\theta, e_\omega) = k_0 e_z + k_1 e_\theta + k_2 e_\omega, \qquad (5)$$

where $e_z = \int_0^t e_\theta d\tau$. Then the proposed method has a decay dynamics, $S(e_z, e_\theta, e_\omega) = 0$. From the derivative of S with respective to time, t

$$\dot{S}(e_\theta, e_\omega, \dot{e}_\omega) = k_0 e_\theta + k_1 e_\omega + k_2 \dot{e}_\omega$$
$$= k_0 e_\theta + k_1 e_\omega + k_2 \dot{\omega}^d - \frac{K_a K_t k_2}{J_m}(u + d). \qquad (6)$$

We design the control input, u with a pure switching component, v by taking

$$u = u_{eq} + v \qquad (7)$$

where

$$u_{eq} = \frac{J_m}{K_a K_t k_2}(k_0 e_\theta + k_1 e_\omega + k_2 \dot{\omega}^d)$$

to cancel the known terms, $k_0 e_\theta + k_1 e_\omega + k_2 \dot{\omega}^d$, on the sling manifold. Substitute (7) for (6), the dynamics of the sliding manifold becomes

$$\dot{S}(e_\theta, e_\omega, \dot{e}_\omega) = K_s(v + d). \qquad (8)$$

Table 1. Plant parameter and controller gain

Parameter	Value	Parameter	Value
K_t	0.187	J_m	$3.1 \times 10^{-4} \mathrm{kg \cdot m^2}$
K_a	1.5385×10^4	k_0	1.02
k_1	17.5	k_2	0.32
ρ	2	T_s	$16.67 \mu sec$
ϵ	0.2		

where $K_s = \frac{J_m}{K_a K_t k_2}$ Suppose that the unknown term d is physically bounded function. Then, we can design nonlinear switching function, v by

$$v = -\rho \mathrm{sgn}(S), \qquad (9)$$

where $\rho \geq |d|$, and its continuous approximation is obtained by replacing sgn(s) by below saturation function, sat($\cdot$).

$$\mathrm{sat}(S) = \begin{cases} 1, & \text{if } S > \frac{1}{\epsilon} \\ -1, & \text{if } S < -\frac{1}{\epsilon} \\ \epsilon S, & \text{else.} \end{cases} \qquad (10)$$

where ϵ is a slope of saturation function and is chosen as a arbitrary positive number. Consider a Lyapunov candidate function, $V(\cdot)$

$$V(S) = \frac{1}{2} S^2. \qquad (11)$$

To ensure that sliding mode $S(e_z, e_\theta, e_\omega) = 0$ is attainted in a finite time, the derivative of $V(S)$ with respect to time needs to be negative definite. $\dot{V}(S)$ is computed as

$$\dot{V}(S) = S\dot{S}$$
$$= -\rho K_s |S|(1 - \frac{d}{\rho}\mathrm{sat}(S)) \qquad (12)$$
$$\leq -\rho K_s |S|\alpha < 0$$

where $\inf_{t \in [0,\infty)} (1 - \frac{d}{\rho}\mathrm{sat}(S)) = \alpha > 0$. If we can design arbitrary large $\rho > \sup_{t \in [0,\infty)} |d(t)| + \eta$ with $\eta > 0$, $\dot{V}(S)$ is negative definite for boundary layer. Therefore, for any initial states there exists a finite time, T_f to ensure reaching condition for boundary layer around sliding manifold (Edwards and Spurgeon (1998)).

Remark 1. For sliding mode control design, reaching condition depends on saturation function gain. Sufficiently large saturation function gain is helpful for satisfaction of the reaching condition. However, it becomes the cause of chattering phenomenon and is difficult to compensate for excessive uncertainty if there exists resonance modes which are excited by such chattering. ◇

3.3 Disturbance Observer Design

For the SMC design, switching function gain ρ depends on uncertainty bound of $|d|$. In the presence of plant uncertainty such as resonance mode, chattering is not negligible. Therefore, it is not practical to use high gain in our application where the first resonance frequency is close to the zero dB crossover frequency. To remedy this problem, we use a disturbance observer (DOB) proposed in (Kang et al. (2011)) to reduce switching function gain. The disturbance estimation by the DOB reduces the switching gain required to guarantee the reaching condition. Let us define the estimated disturbance, $\hat{d}$

$$\hat{d} = d - \tilde{d}, \qquad (13)$$
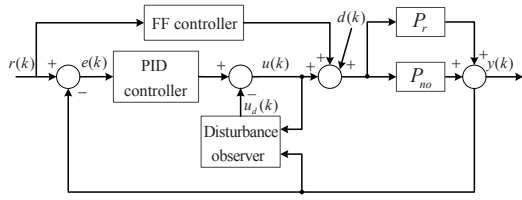
Fig. 4. Block diagram of conventional Feedfor-
ward+PID+DOB
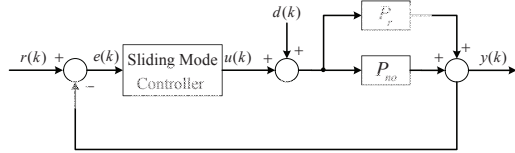
Fig. 5. Block diagram of conventional SMC
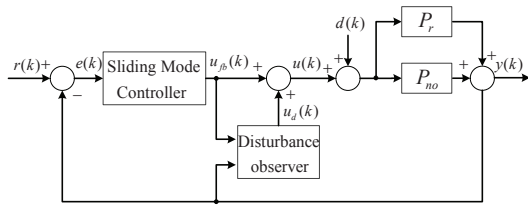
Fig. 6. Block diagram of proposed SMC with DOB

where $\tilde{d}$ is disturbance estimation error and redefine the control input, u using $\hat{d}$ as

$$u = u_{eq} - \hat{d} + v. \tag{14}$$

Then (12) can be reformulated as

$$\dot{V}(S) = S\dot{S}$$
$$= -\rho K_s |S|(1 - \frac{\hat{d} - d}{\rho}\text{sat}(S)). \tag{15}$$

Assumption 2. Suppose that given the closed-loop system is stabilized. If the DOB is well designed and implemented, the supremum of the absolute value of disturbance estimation error

$$\tilde{d}_{max} := \sup_{t \in [0,\infty)} |d(t) - d\hat{(t)}| \tag{16}$$

exists. ◇

In this application Assumption 2 is reasonable since we know that $|d(t)|$ is bounded as long as the closed-loop system is stabilized. If the condition $\rho > \tilde{d}_{max} + \eta$ is satisfied, the finite time reaching condition of the SMC is achieved. With well designed DOB it is clear that

$$\tilde{d}_{max} << \sup_{t \in [0,\infty)} |d(t)|$$

so that a relatively small switching gain with DOB can be used as long as trajectory stay around the sliding manifold.

Remark 3. For the compensation of the unknown uncertainty arisen by viscous damping and flex cable, selecting a high switching function gain is not practical. Therefore, bias compensation by using the DOB is helpful to meet the reaching condition without excessive high switching function gain. ◇
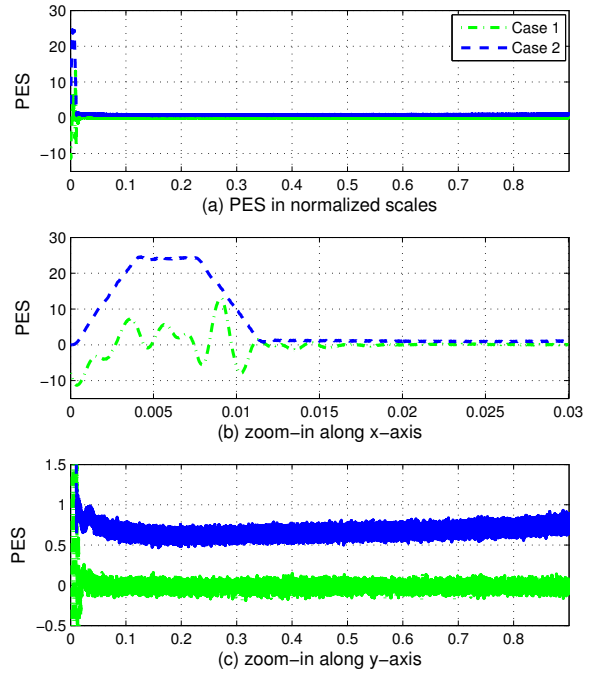
Fig. 7. PES of Case 1 and 2 - (a) PES in normalized scales, (b) zoom-in along x-axis, (c) zoom-in along y-axis
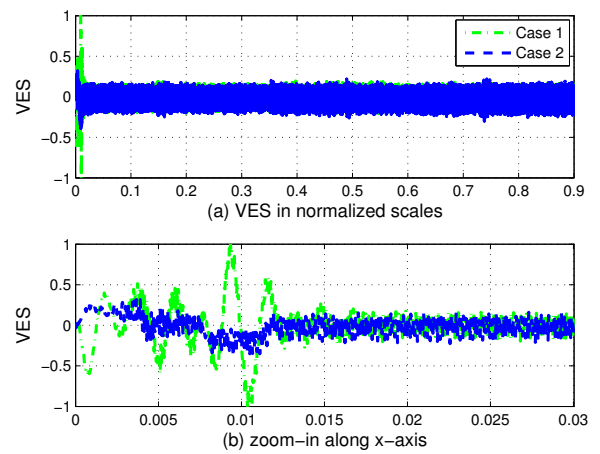
Fig. 8. VES of Case 1 and 2 - (a) VES in normalized scales, (b) zoom-in along x-axis

4. APPLICATION RESULTS

We performed experiments to evaluate the performance of the proposed control scheme with a Digital Signal Processor with the sampling time, T_s. The plant parameters and controller gains listed in Table 1 were used. The velocity profile for spiral track writing shown in Fig. 3 is used. The position profile is generated from an integration of the velocity profile. To verify the performance of the proposed control scheme, three cases were studied.

- Case 1: conventional PID controller with DOB,
- Case 2: conventional SMC,
- Case 3: proposed SMC with DOB.
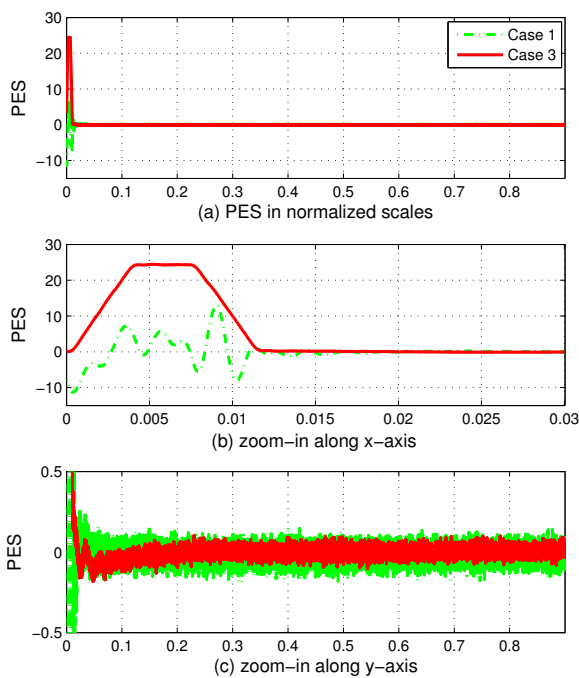
Fig. 9. PES of Case 1 and 3 - (a) PES in normalized scales, (b) zoom-in along x-axis, (c) zoom-in along y-axis
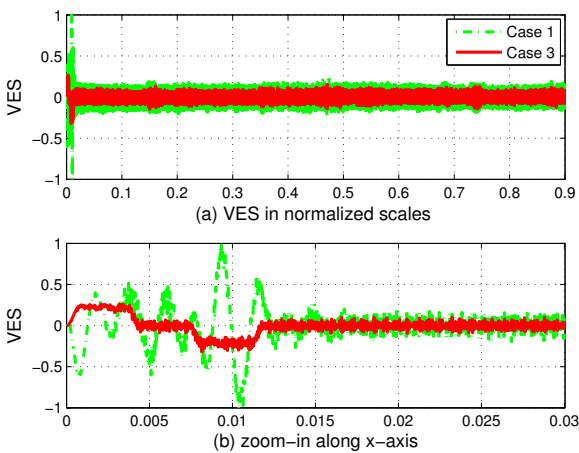
Fig. 10. VES of Case 1 and 3 - (a) VES in normalized scales, (b) zoom-in along x-axis

Figure 4, 5, 6 are block diagrams of the Case 1, and Case 2, and Case 3, respectively. The conventional DOB implemented by using ZPET (Tomizuka (1987)) is used for Case 1. The add-on type DOB (Kang et al. (2011)) is used to estimate plant uncertainties. For simple comparison of the three cases, scaled experiment results are provided.

4.1 Comparison of Case 1 to Case 2

PES and VES of Case 1 and 2 are plotted in Figs. 7 and 8, respectively. From the zoomed x-axis plots of both PES and VES, it looks like that fast settling time is achieved with only SMC since undershoot of Case 2 is not noticeable. In Fig. 7 (c), however, offset of PES for
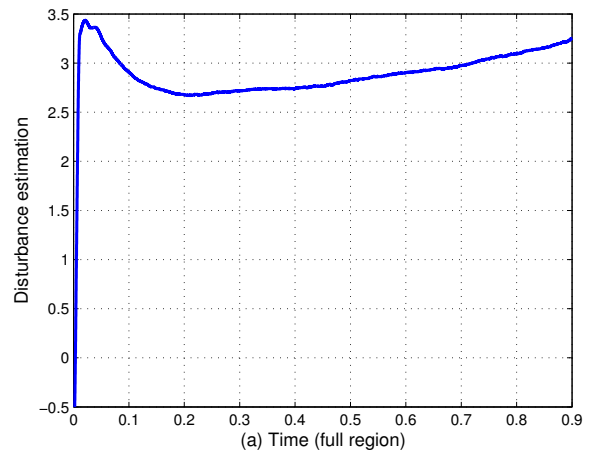
Fig. 11. Destimated disturbance
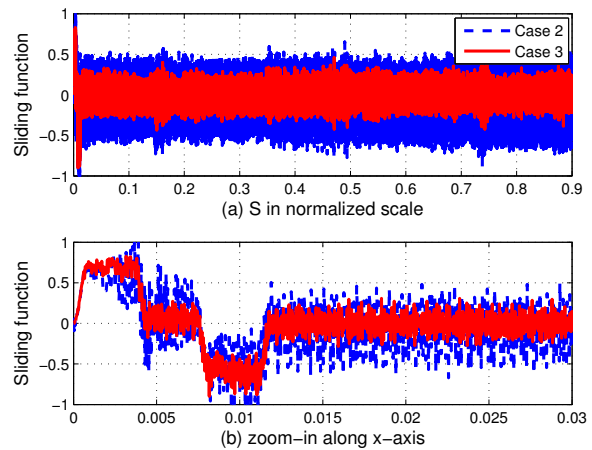
Fig. 12. Sliding functions of Case 2 and 3 - a) S in normalized scale, (b) zoom-in along x-axis

Case 2 during constant velocity region appears. It resulted from the plant uncertainties because we did not select a sufficiently large switching gain. We have experienced that increasing the switching gain does not necessarily reduce the amplitude of PES and its offset. It was observed in this application that high switching gain to reduce the offset of PES may cause the servo system unstable due to excitation of the resonance modes. Thus, it is not practical blindly to use high gain for switching function. In Fig. 8 (b), we observed that oscillation in VES of Case 1 entails a longer settling time to constant velocity region. On the other hand, VES of Case 2 does not show such such a oscillation and its shape is similar to the jerk profile in acceleration and deceleration region. In the next section, we will show effect of DOB on bias compensation.

4.2 Comparison of Case 1, 2 and 3

Position and velocity tracking performances of the Case 1 and 3 are shown in Figs. 9 and 10. In Fig. 9 (b), (c), we see that most of PES offset during the constant velocity region is removed due to the effect of DOB. The estimated disturbance is plotted in Fig. 11. Also a fast settle time is obtained. Amplitudes of both PES and VES of Case 3
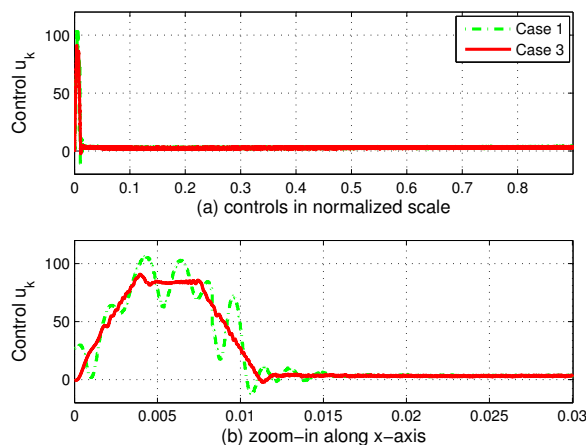
Fig. 13. VCM input of Case 1 and 3 - (a) controls in normalized scale, (b) zoom-in along x-axis

are also reduced compared with the other cases. Thus it turns out that the add-on type DOB is very effective in bias compensation in regulation via integral SMC. Sliding functions of Case 2 and 3 are plotted in Fig. 12. The trajectories stay near the sliding manifold in the constant velocity region. On the other hand, before reaching the constant velocity region we see that the trajectories of Case 2 and 3 are pushed away from the sliding manifold due to the jerks applied to the system. In spite of the same switching gain, sliding function of Case 3 has a smaller band of PES than that of Case 2. Input currents used in VCM are illustrated in Fig. 13. In the transient region, input torque oscillation of Case 3 is less than that of Case 1. Histograms of PES for the three cases are shown in Fig. 14. One can observe that PES histogram of Case 2 has a bias. However, the PES of Case 3 is densely distributed around zero compared to other cases. Frequency spectrum of the position error signals are illustrated in Fig. 15. Applying the add-on DOB reduced frequency spectrum magnitude error in low frequency region as well as high frequency region.

5. CONCLUSIONS

In this paper, we proposed the new control scheme for spiral servo track writing. To achieve the fast settling time the integral-type sliding manifold with disturbance observer was developed. In constant velocity region, both position error signal and velocity error signal were well controlled even before the head reaches the constant velocity region. Comparative study with the conventional control method was made. Experiments were performed to verify the effectiveness of the proposed sliding mode control with disturbance observer.

ACKNOWLEDGEMENTS

REFERENCES

D. Abramovitch and G. F. Franklin. (2002) A brief history of disk drive control. *IEEE Contr. Syst. Magn.*, vol. 22, no. 3, pp. 28-42, Jun. 2002.
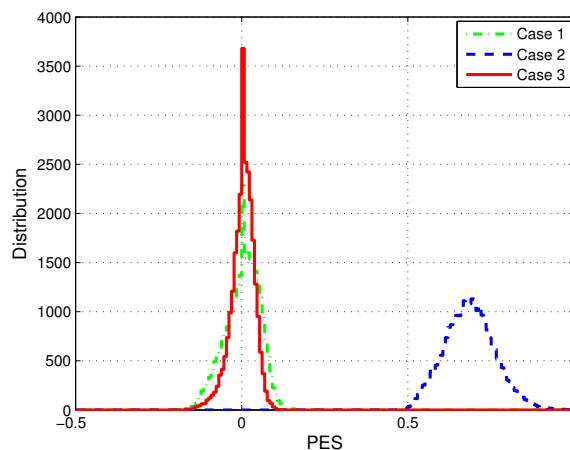
Fig. 14. Histogram for PES of Case 1, 2 and 3
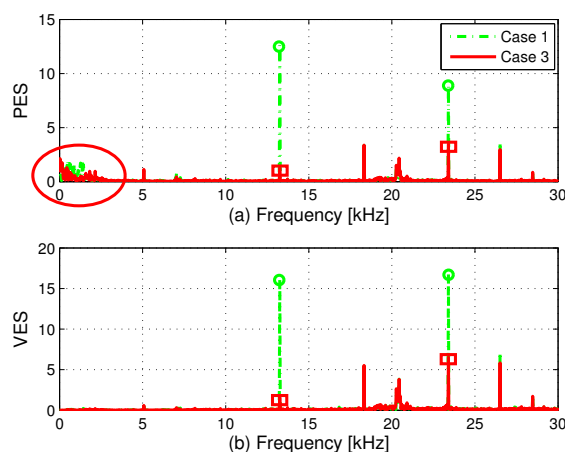
Fig. 15. Frequency spectrums for PES of Case 1 and 3

A. A. Mamun, G. Guo, and C. Bi. (2007) Hard Disk Drive Mechatronics and Control. *CRC Press*, 2007.

T. Yamaguchi, M. Hirata, and J. C. K. Pang. (2011) High-speed precision motion control. *CRC Press*, 2011.

S. H. Kim, S.-H. Lee, and C. C. Chung. (2013) Minimizing Residual Vibration With Resonance Filter for Nonminimum-Phase Plants. *IEEE Trans. on Magn.*, vol. 49, no. 6, 2013.

M. Tomizuka. (1987) Adaptive Zero Phase Error Tracking Algorithm for Digital Control. *ASME, J. Dynam. Syst. Meas. Contr.*, vol. 109, no. 1, 1987.

H. J. Kang, K.-S. Kim, S.-H. Lee, and C. C. Chung. (2011) Bias compensation for fast servo track writer seek control. *IEEE Trans. on Magn.*, vol. 47, no. 7, July. 2011.

C. Edwards and S. K. Spurgeon. (1998) Sliding mode control, theory and applications. *Taylor & Francis Ltd*, 1998.

H. K. Khalil. (2002) Nolinear systems. *Pearson Education*, 2002.